Application of soil-cement columns for better seismic design of bridge piles and mitigation of nearby ground vibration due to traffic

Hirokazu TAKEMIYA*, Jorge SHIMABUKU**

* Dr. of Eng., Professor, Dept. of Env. and Civil Eng., Okayama University, Tsushima Naka 3-1-1, Okayama 700-8530
** Ph.D., Research Fellow, Dept. of Env. and Civil Eng., Okayama University, Tsushima Naka 3-1-1, Okayama 700-8530

This paper investigates an improved soil-pile foundation-bridge system by the surrounding soil columns against earthquake motions and a honeycomb shaped WIB (Wave Impeding Barrier) measure for reduction of traffic-induced vibration. Focusing on these different types of vibrations of a highway bridge, a parameter studies are conducted for the development of the better design. The time domain FEM-BEM method is used for both analyses. From the results, the advantages of soil improvement are interpreted for the seismic problem and of the honeycomb WIB for the paraseismic problem.

Key Words: soil improvement, pile foundation, vibration mitigation, honeycomb shaped WIB seismic problem, traffic-induced vibration

1. Introduction

Pile foundations are widely used to transfer axial structural loads through soft soils to stronger bearing strata at depth. Structures sited on soft soils are founded by deep foundations. Those are also demanded on the lateral resistance against earthquake loading, especially for highway bridges as has been evidenced in recent strong earthquakes. However, it may be costly to have a sound design and construction of pile foundation at very soft soil sites due to its low horizontal bearing capacity. Another implicit and important problem in very soft soil sites is the vibration transmission by traffic from highway bridges to the surrounding soil. The term "paraseismic" is used to address this problem in contrast to the seismic problem for natural earthquake sources. The induced ground vibrations, even if not damaging to nearby structures, are annoying to residents alongside. It may also have unfavorable effects on high-technology facilities. The development of counter measures against such vibration problems is therefore of big importance.

In the seismic design, improving soil partially where the piles are embedded at soft soil is an effective measure alternative to increase the horizontal resistance and reduce the environmental vibrations. Recently static loading tests were conducted[1] to investigated this measure.

From the vibration point of view of a structural and the nearby ground due to certain loading on the structure, the investigation should also be addressed to reduce those responses. Traditionally, open or filled-in trenches or concrete walls are typical measures used. The Wave Impeding Barrier (WIB) is another type of measure based on the wave cut-off frequency of the medium[2]. The recent development is the honeycomb shaped WIB[3]. The construction practice for the honeycomb WIB is the cement mixing procedures into the soft ground. These vertical soil-cement column systems are arranged in shape of honeycomb to constraining and blocking the soil motions due to the propagating waves.

In this paper, a typical bridge supported by piles of the Japanese Highway network is analyzed to investigate the effectiveness of soil improvement-pile foundation system against seismic sources. Moreover, the characteristics of wave propagation in surrounding soil and effectiveness of the honeycomb WIB countermeasure are investigated.

2. Methodology of analysis

The analysis is made using the two-dimensional (2-D) time domain FEM-BEM (Finite Element Method-Boundary Element Method) hybrid technique[4]. This hybrid method utilizes advantages of the respective discretization methods; namely, FEM accommodates the structure and the near part of non-homogeneous soil with complicated material properties, while the BEM fulfills the infinitely extending boundary condition. In this research, the FE region is considered as a

nonlinear zone for the seismic analysis and linear for the paraseismic analysis in view of the induced strain levels. The BE region is considered as linearly elastic domain for both analyses. Therefore, the deeper stiff soil is included in the BE zone, the pier and piles are discretized by beam elements, the neighboring soil by FEM and the vertical boundary is located at far distance from the area of interest. Moreover, fictitious high damping coefficients are imposed to the FE soil edge elements in order let them absorb the outgoing waves.

For the nonlinear analysis, the inelastic behavior of RC beam elements are represented by the one component model proposed by Giberson[5] with the consideration of both sway and rotational motion at both ends of each element as presented by Takemiya and Shimabuku[6]. The RC hysteresis model is treated by the Q-hyst model[7], which was modified to take into account of the relationship between bending moment and axial force[8]. The axial load is considered in the evaluation of the yield bending moment at each computational step from the bending moment-axial force interaction diagram. The soil nonlinear behavior is characterized by the Mohr stress circle criterion and the hyperbolic model originally proposed by Hardin and Drnevich[9], which was refined by Takemiya *et al.*[10] to be more suitable for computational simulation in 2-D problems for irregular seismic loading. The equation of motion of the total system is solved step-by-step by the Newmark method by taking care of the nonlinearity by the Newton-Raphson procedure.

3. Properties of studied case

Fig.1 is an illustration of a typical bridge of the Japanese highway bridge and the model for analysis, where the rows of piles are denominated as 1, 2, 3 and 4 for reference. The length of pile elements is taken the same with the size of soil elements. The BEM boundary is located at G.L. –21.5 m and the vertical side boundaries are located at 83.75 m from the center of footing. In order to meet with the plane strain assumption for the FE soil model, a compatible beam for this assumption should be considered by taking a properly chosen distance in the third direction. No appreciable influence exists from the region beyond 2W, in which W is defined for footing width concerned. This is based on the same consideration for piles design procedure[11]. The width of 24 m (twice width of the footing) is adopted in the third direction herein. The site is a two-layered a soil deposits; the surface layer is denoted by LAYER I and the underlain much stiffer soil by LAYER II. The LAYER I is a very soft soil with the thickness of 17 m, the shear velocity of 100 m/s, the mass density of 1500 kg/m^3, the Poisson's ratio of 0.45 and the damping ratio of 0.05. The LAYER II is assumed to have the same properties of the elastic extending half-space (BE) with the shear velocity of 600 m/s, the mass density of 1800 kg/m^3 and the Poisson's ratio of 1/3. The properties of the RC pile and pier are given in **Table 1** and **Table 2**.

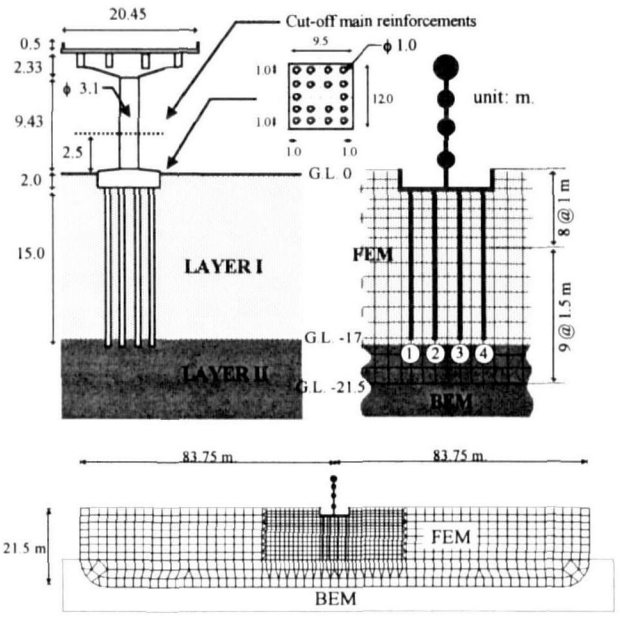

Fig.1 Typical bridge of the Japanese Highway network and its model of analysis.

Table 1 Properties of concrete

Compressive strength, σ_{ck} (Pa)		2.7×10^7
Modulus of elasticity, E_c (Pa)		2.8×10^{10}
Strain under maximum compression stress, ε_{cc}	Pier below 2.5 m of height	4.26×10^{-3}
	Pier above 2.5 m of height	2.89×10^{-3}
	Pile	3.00×10^{-3}
Ultimate strain of restrained concrete, ε_{cu}	Pier below 2.5 m of height	5.80×10^{-3}
	Pier above 2.5 m of height	3.42×10^{-3}
	Pile	3.59×10^{-3}

Table 2 Properties of reinforcement

Yield strength, σ_{sy} (Pa)				3.5×10^8
Modulus of elasticity, E_s (Pa)				2.1×10^{11}
Longitudinal bars	Pile	Number		18
		Diameter (mm)		29
	Pier	Below 2.5 m of height	Number	180
			Diameter (mm)	35
		Above 2.5 m of height	Number	120
			Diameter (mm)	35

4. Seismic analysis of bridge supported by pile foundation embedded in improved soil

The original soil showed in **Fig. 1** is improved to the configuration and dimensions of **Fig. 2**. The model with no measure (**Fig. 1**) is denoted Case A, the model with 12 m horizontal length of improved soil (**Fig. 2a**) is Case B and the model with 17 m horizontal length (**Fig. 2b**) is Case C. The soil

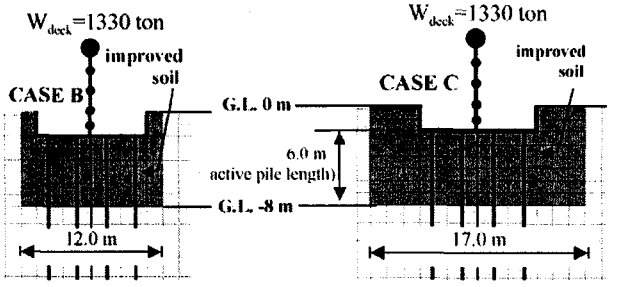

(a) Case B (b) Case C

Fig.2 Improved soil cases for the seismic analysis.

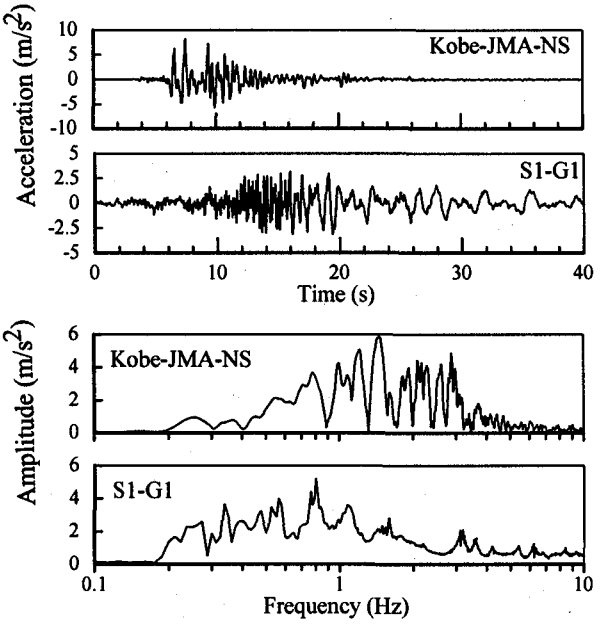

Fig. 3 Kobe-JMA-NS and S1-G1 input records.

improvement depth is determined by the pile active length $1/\beta$. This active length calculated according the Japan Road Association[11] is 6 m for a pile with diameter of 1 m embedded in homogeneous stratum of Vs=100 m/s (see **Fig. 2**). The equivalent properties of the improved soil for the 2-D in-plane analysis are defined as shear velocity of 300 m/s, mass density of 2000 kg/m^3, Poisson's ratio of 0.4 and damping ratio of 0.05.

After the 1995 Hyogo-ken Nanbu earthquake, the Japanese codes were revised to take into account of devastating earthquake motions such as observed in addition to the ordinary earthquake motions that have been used for earthquake resistant design so far. These two types of earthquake excitations are determined as Type II ground motions according to the Japanese Design Specification of Highway Bridges, Part V[12]. Herein, North-South component of the 1995 Hyogo-ken Nanbu Earthquake record in Kobe (JMA-NS) is used as representative of the Type II ground motion. Moreover, an artificially generated motion is considered from the spectrum matching for a typical near-source earthquake. It is called the S1-G1, which corresponds to motion on ground 1 (bedrock) of Level II-Spectrum I of the Japanese Seismic Design Code for

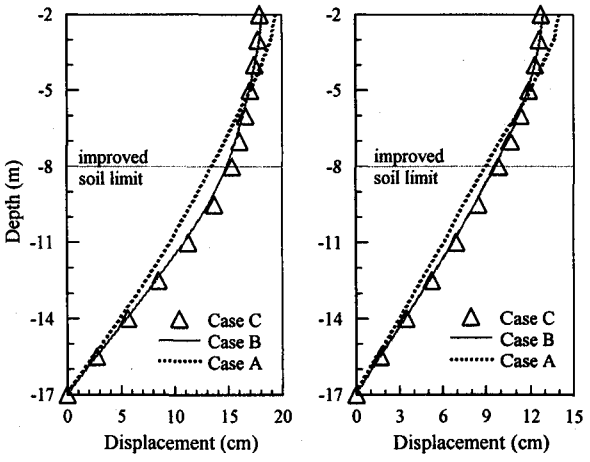

(a) For Kobe-JMA-NS (b) For S1-G1

Fig. 4 Maximum displacement distribution along the pile length for both input records.

Railway Structures[13]. The time histories and Fourier spectrum are depicted in **Fig. 3**. While, the spectral densities are concentrated in the high frequency range for the Kobe-JMA-NS record, the maximum amplitudes correspond to low frequency range for the S1-G1 motion. The predominant frequencies are respectively 1.46 Hz and 0.8 Hz for the Kobe-JMA-NS and S1-G1 motions. The displacement input is imposed at G.L. –100 m in order to expect a reliable solution from the computational model. The time step interval at BE zone (Δt_{BE}) is assumed equal to the input record, namely 0.02 s for the Kobe-JMA-NS record and 0.04 s for the S1-G1 record. The incremental BE time step (Δt_{BE}) is divided into 16 smaller time steps to define the time step interval at FE zone (Δt_{FE}). For all cases, the nonlinear behavior of soil and structure is considered.

Fig. 4 shows the maximum horizontal displacement distribution along the pile length. These pile displacements were chosen as the maximum of all piles. From this figure, it is noted that the soil improvement reduces the pile top horizontal displacements. However, the displacement increases at deeper zones, where the piles are only constrained by the soft soil. When the soil improvement is not considered, the pile displacement follows the free-field soil horizontal displacements in average sense[14]. However, in the Case B and Case C, the deviations between G.L. –5 m and G.L. –11 m, especially at soil improvement limit (G.L. –8 m in **Fig. 2**), reflect the different boundaries. Moreover, most of the amplification occurs at soft soil with almost uniform slope in the improved soil zone.

Fig. 5 shows the maximum bending moment distribution along the pile length, where the yield bending moment under static axial load (vertical line) is included for reference. These bending moments were chosen from the maximum of all piles. When the soil is improved (Case B and Case C), the bending moment is reduced significantly near the pile top. This behavior is more remarkable for the Case C since the rotational constraint

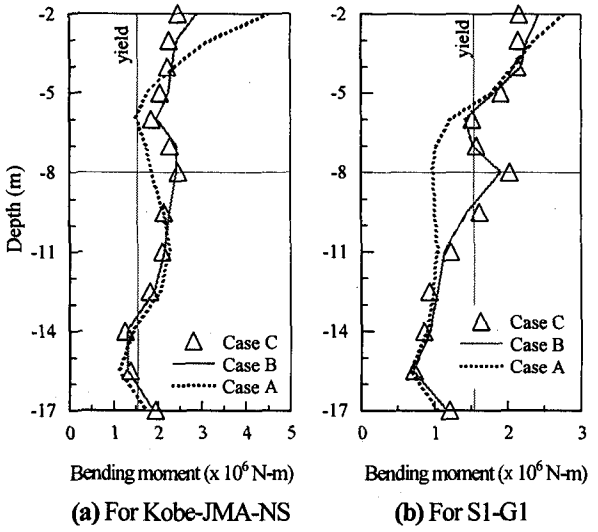

Fig. 5 Maximum bending moment distribution along the pile length for both input records.

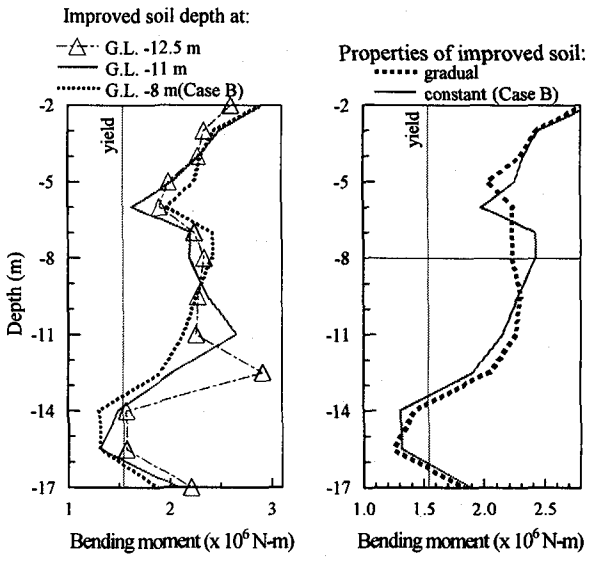

Fig. 6 Maximum bending moment distribution along the pile length for Kobe-JMA-NS excitation.

provided by the large horizontal length of soil improvement (17 m) renders the rocking component of improved soil block smaller than for the Case B. On the other hand, the soil improvement leads to large bending moments around G.L. –8 m, which corresponds to the boundary zone between the improved soil and the soft soil. The maximum bending moments at boundary zone for cases B and C have the same values that at the pile top. This composed soil-pile foundation system has a similar behavior to that of a caisson foundation and consequently the bending moment is increased at the soil improvement depth. From above considerations, it is noted that the improved soil depth is an important factor for the pile behavior. Moreover, in the case of piles supported at bearing bottom layer, the length of pile below the soil improvement should be adequate to avoid "short pile" type problems. **Fig. 6a** shows the bending moment distribution for different soil improvement depths: G.L. –8 m (Case B), G.L. –11 m and G.L. –12.5 m. These depths are chosen to cover the range between $1/\beta$ and $\pi/2\beta$, which is the improvement depth proposed by the Japan Highway Technical Center[15]. From this figure, large bending moments are noted at G.L. –11 m and G.L. –12.5 m. The bending moment at G.L. –12.5 m is larger than at pile top, which is an undesirable behavior. An effective way to reduce the bending moment at these boundaries is to make a smooth variation of the pile deformation with depth, eliminating an abrupt change at the boundary of different soil properties. The soil column installation by cement injection in the neighborhood of piles is a possible procedure. In **Fig. 6b**, the Case B is compared with a case, which is improved until the same depth, but changing its properties proportionally with the depth from G.L. –5 m (inflection point of pile) to G.L. –8 m. While the pile top bending moment practically not modified, a reduction is appreciated at G. L. –8 m. Further studies and laboratory experiments are necessary to develop this idea for its

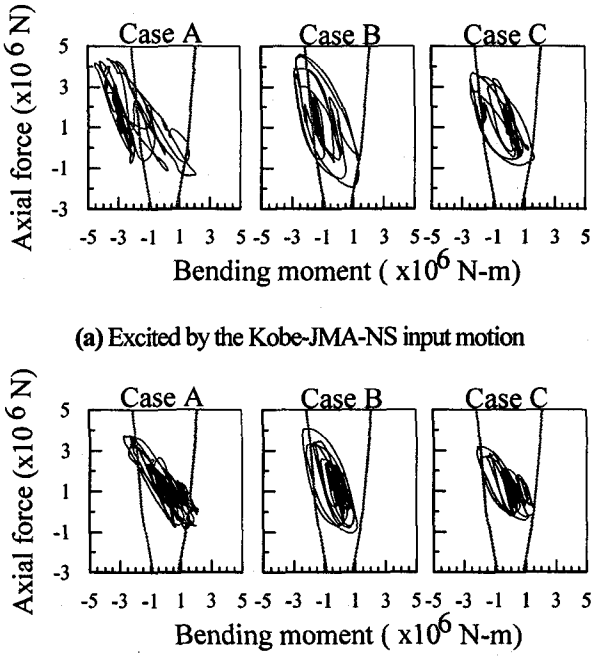

Fig. 7 Bending moment-axial force relationship at top of pile 4.

engineering application.

In **Fig. 7**, the relationship between the axial force (positive value for compression) and bending moment is investigated at top of pile 4 (defined in **Fig. 1**). This pile experiences the maximum compression force, which includes the initial static axial force. Since the possible failure of the pile is due to the relation between compression force and bending moment rather than tension force-bending moment relationship[14], the soil improvement of Case C leads to considerably reduction of the inelastic behavior.

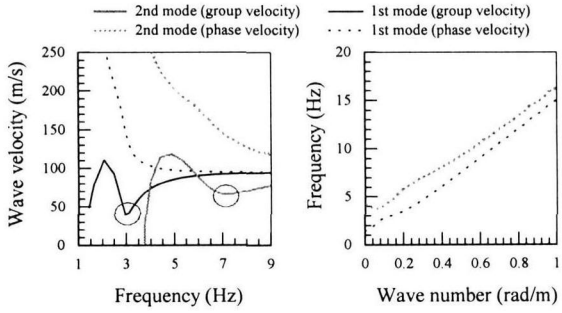

Fig.8 In-plane dispersion curves of soil.

Table 3 Results of modal analysis.

Superstructure fixed at its base	Whole system (superstructure-pile footing-soil)			
F (Hz)	Mode	Participating mass (%)		F (Hz)
		X-dir	Z-dir	
1.94	1	77.61	—	1.44
	2	16.26	—	4.52
	3	—	83.58	11.58

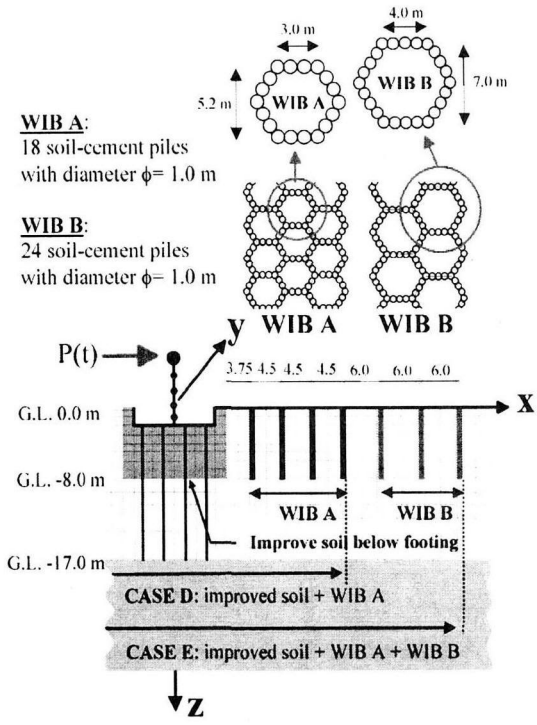

Fig. 9 Honeycomb WIB dimensions and its idealization.

5. Paraseismic analysis and vibration mitigation by honeycomb WIB

In the paraseismic analysis, the engineering focus is placed on the response features of the nearby soil. In order to predict the dispersive wave motions at the site, relationships between the propagation wave velocity, frequency and wave number are depicted in **Fig. 8**. When a soil stratum is loaded by an impulse, then the stratum tends to show a transient response; the first phase is associated with it then followed by the motions that depend on the soil properties. The group velocity of wave propagation gives an information on the Airy phase at the local minimum values. It is noted that the Airy phase appear in the low modes of in-plane motion at 2.9 Hz and 7.2 Hz, as marked by circles in the figure; therefore, the wave motions travel most at these frequencies. Natural frequencies and participating masses for the bridge-footing-pile-soil system are given in **Table 3**. The fundamental frequencies are calculated by the stick modeling, where the soil reaction springs are assumed according to the Japanese Design Specification of Highway Bridges, Part IV[11]. The first mode of whole system (77.61% participating mass) represents the pier top horizontal motion. The table also includes the fundamental frequency (1.94 Hz) of bridge structure with a fixed condition at its base.

The authors propose the honeycomb shaped WIB as measure for induced vibration from highway bridge supported by piles. For the studied case, the honeycomb dimensions and the model for analysis are depicted in **Fig. 9**. Two honeycomb WIBs are considered: a WIB A and a WIB B with 18 and 24 soil-cement columns respectively of a diameter 1.0 m. In order to evaluate the effectiveness of the honeycomb WIBs, the previously presented Case A and Case B are used for comparison. The cases for the vibration mitigation analysis consider the improved soil below the footing with the honeycomb WIB A (Case D in **Fig. 9**) and the improved soil below footing with the honeycomb WIB A and WIB B (Case E in **Fig. 9**). The horizontal length of honeycomb WIB of Case D corresponds roughly to the half wavelength (17 m) and for the Case E to one wavelength (34 m). This wavelength corresponds to the wave propagation in first Airy phase frequency of 2.9 Hz. The vertical length of honeycomb WIBs is equal to the depth of the improved soil below the footing. The shear velocity of soil-cement piles is 500 m/s, the mass density is 2000 kg/m^3, the Poisson's ratio is 0.4 and the damping ratio is 0.05. Since the plane strain condition is assumed with a width of 24 m in the y-direction, the soil-cement piles in x-direction are idealized by truss elements considering their equivalent longitudinal area in this 24 m. The external loads P(t) are applied at pier top in x-direction as showed in **Fig. 9**. Only the horizontal direction is analyzed since the predominant amplifications were observed in the field measurements[16]. Since the behavior of nearby soil depends on the frequency characteristics of input loading, bridge and soil; the loading frequencies are chosen as 1.4 Hz, 2 Hz, 2.5 Hz and 3.3 Hz. **Fig. 10** depicts the loading time functions and their Fourier amplitudes used in the analysis. These loadings correspond to an impulsive one Ricker wavelet type loading (**Fig. 10a**), harmonic sine wave function (**Fig. 10a**) and a series of Ricker wavelets (shown in **Fig. 10a**) that can overlap with the succeeding waveforms in phase for frequencies of 1.4 Hz, 2.0 Hz, 2.5 Hz and 3.3 Hz. The superposition of Ricker wavelets is used because of its simple form and good analytical properties. These overlapping Ricker wavelets are shown in **Fig. 10b**.

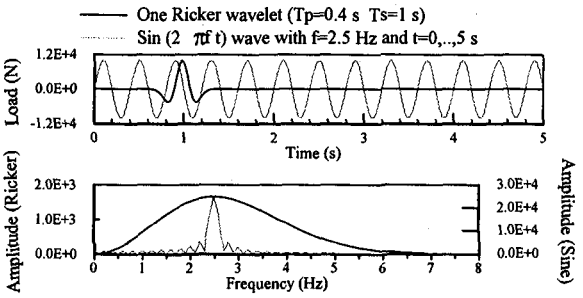

(a) One Ricker wavelet and Sine wavelet

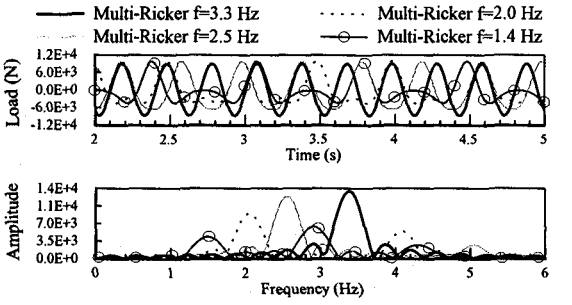

(b) Series of Ricker wavelets

Fig. 10 Loading functions.

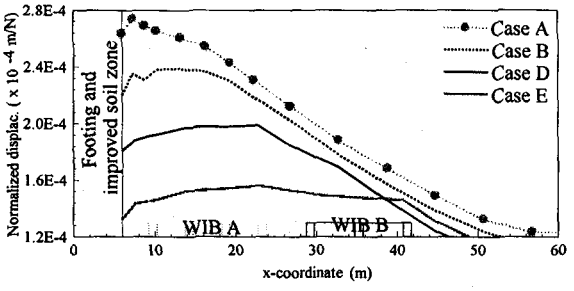

(a) For one Ricker wave type loading (f=2.5 Hz)

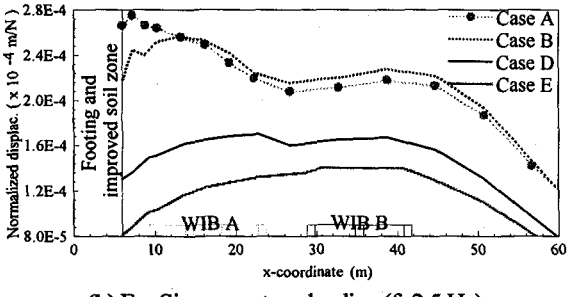

(b) For Sine wave type loading (f=2.5 Hz)

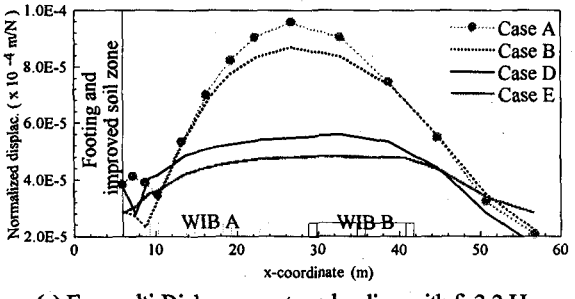

(c) For multi-Ricker wave type loading with f=3.3 Hz

Fig. 11 Maximum horizontal displacements at surface (continue)

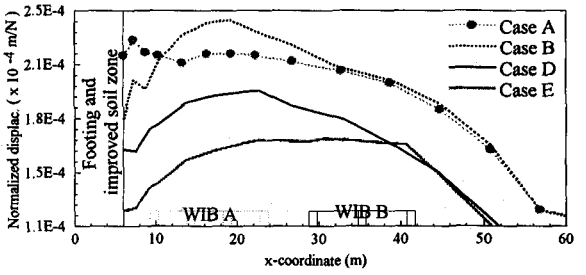

(d) For multi-Ricker wave type loading with f=2.5 Hz

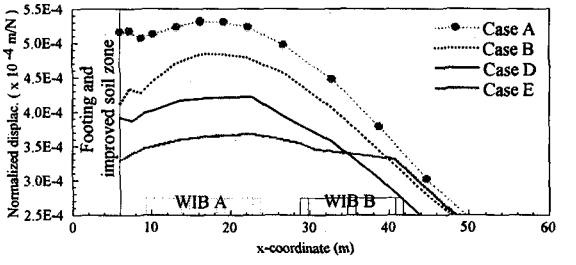

(e) For multi-Ricker wave type loading with f=2 Hz

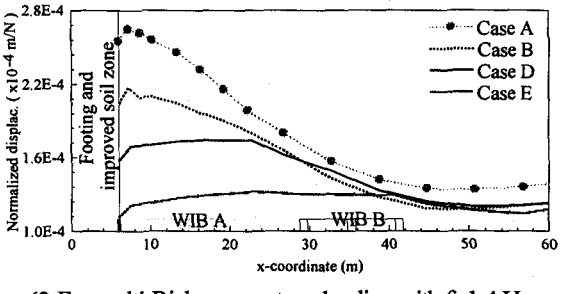

(f) For multi-Ricker wave type loading with f=1.4 Hz

Fig. 11 Maximum horizontal displacements at surface.

Fig. 11 shows the maximum surface horizontal displacement response for all the cases. These computation results are depicted in normalized form (the maximum displacement divided by maximum horizontal loading). For the series of Ricker wavelet type loadings, the would-be steady state maximum responses are chosen from 2 s to 5 s in the duration, which corresponds to loading time showed in **Fig. 10b**. The reduction effect by the honeycomb WIB is appreciably noted at ground above the WIB location. If **Fig. 11a** and **Fig. 11b** are compared, the differences between the response due to impulsive and harmonic loadings are clearly noted. This also can be seen in **Fig. 13** for their respectively time histories. For the harmonic sine wave type loading (**Fig. 11b**), the cases without honeycomb WIB (Case A and Case B) show a second local peak around x=40 m. This distance coincides approximately with the wavelength at the site. On the other hand, for the impulsive one Ricker wave type loading (**Fig. 11a**), the maximum displacements at x= 40 m are practically the same for all cases since the response decreases proportionally with the distance from the bridge structure. Obviously, the reduction effect of Case E is better than the Case D since its mitigation area is larger than Case D. It indicates that the soil behavior is

completely different by loading type, impulsive or harmonic. If the responses due to harmonic loadings constructed from series of Ricker waves are compared (**Fig. 11c** to **Fig. 11f**), the displacements of Case A and Case B are practically the same for f=2.5 Hz (**Fig. 11d**) and f=3.3 Hz (**Fig. 11c**). On the other hand, the values near the structure for both cases varies for f=1.4 Hz (**Fig. 11f**) and f=2 Hz (**Fig. 11e**) loadings. Therefore, it confirms that the soil improvement change the frequency characteristics of emitted waves from the pile foundation. Since the system of Case A have a fundamental frequency of 1.44 Hz (see **Table 3**) and of the Case B is approximately 1.94 Hz (if the structure is assumed as fixed at its base), the system filters the responses for these frequencies. Therefore, in the situation of loading frequency is equal (or lower) to system fundamental frequency, soil amplifications at large distances from structure do not appear. By contrast, the loads are "directly" transmitted to surrounding soil for the f=2.5 Hz and f=3.3 Hz loadings. Consequently, the emitted waves from the structure include frequencies close to the first Airy phase frequency of soil, which leads to vibration amplification even at large distance from structure. With respect to horizontal WIB length, if the honeycomb WIB horizontal length is insufficient to cover the distance until where the soil resonance is important (Case D), response amplifications can appear before the honeycomb WIB mitigation zone. The honeycomb WIB impedes the propagation of vibrations into the neighborhood "cutting" in partial form the wave frequencies contents. However, if its length is insufficient, the remaining frequencies can rise up again beyond the position of the mitigation measure and vibration amplification can appear at farther distances. The maximum values of response for Case A and Case B are observed for f=2 Hz, which is due to nearby fundamental frequency of the structure and of the loading.

Fig. 12 shows the maximum horizontal displacement profile along the vertical direction. Due to presence of soil improvement below the footing, a practically equal displacement is observed from G.L. 0 m to G.L. –8 m at x=6m (horizontal limit of improved soil below footing) for a single Ricker waveform loading. For a harmonic sine waveform loading, the maximum displacement of Case B appears at G.L. –8 m. For all cases, the displacement is drastically reduced above this depth. Consequently, the depth of honeycomb WIB should be assumed equal to soil improvement depth as minimum length to prevent the wave propagation below the honeycomb WIB. **Fig. 13** shows the displacement time histories and their corresponding Fourier amplitudes. For a single Ricker waveform loading, the peaks of Fourier spectrum of Case A are located around 1.8 Hz and 2.1 Hz. These frequencies are close to the fundamental frequency of structure and loading. However, the Case E gives one peak only at 2.1 Hz since its fundamental structural frequency is also around 2 Hz. For the other loadings, this characteristic behavior is not noted due to their short frequency range (see **Fig. 10b**).

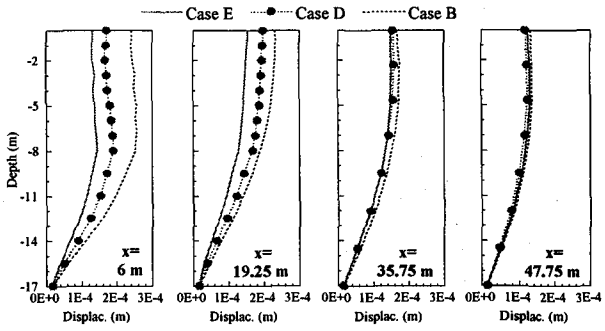

(a) For one Ricker wave type loading

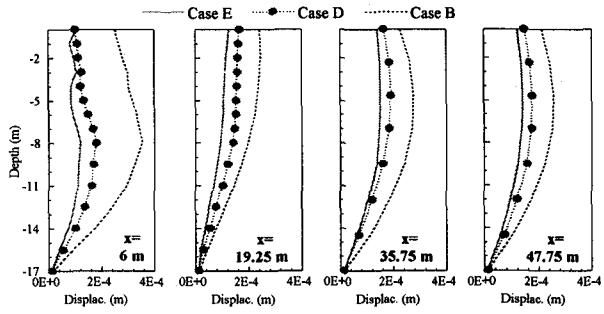

(b) For Sine wave type loading

Fig. 12 Maximum horizontal displacement versus depth.

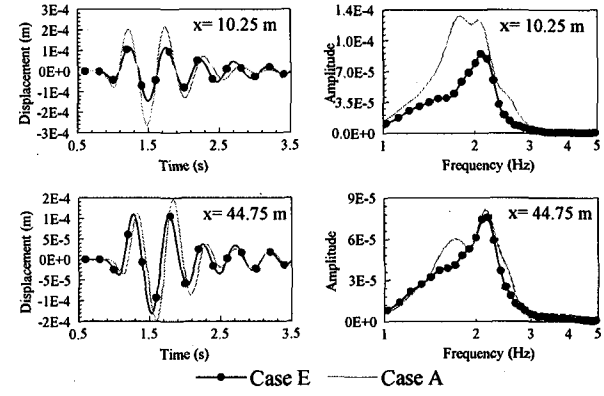

(a) For one Ricker wavelet loading

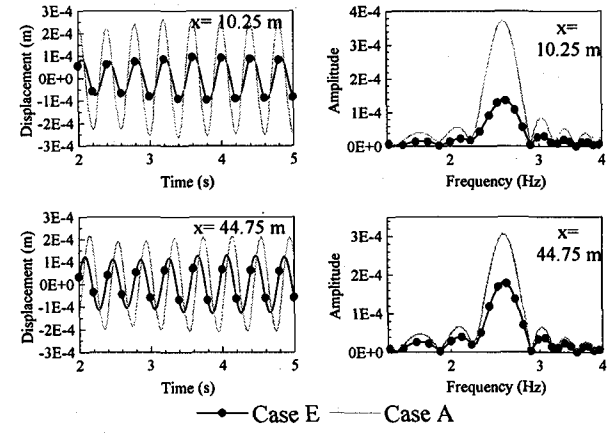

(b) For Sine wavelet loading

Fig. 13 Response time histories and Fourier amplitudes. (continue)

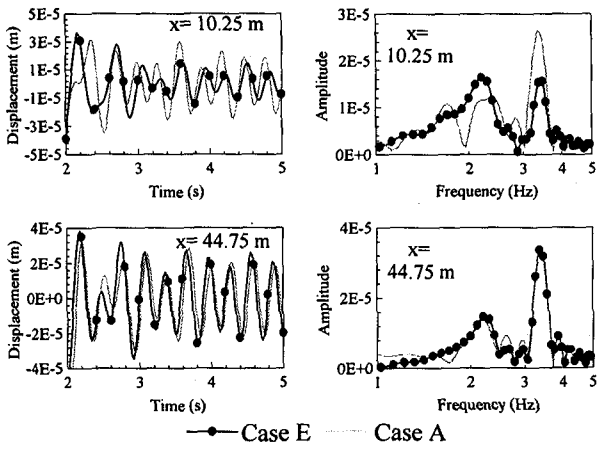

(c) For multi-Ricker wave type loading with f=3.3 Hz

Fig. 13 Response time histories and Fourier amplitudes.

6. Conclusions

In this paper seismic and paraseismic problems have been dealt with a highway bridge at soft site with focuses on the soil improvement-pile foundation system and the surrounding ground vibration reduction by honeycomb WIBs.

In the seismic analysis, the soil improvement around piles leads to a significant reduction of bending moment and displacements at pile top. However, special cares should be paid to the soil improved depth, because large bending moments at its boundary can appear with same or larger magnitudes than at the pile top. Moreover, the length of pile below the soil improvement should be adequate to avoid "short pile" type problems in the case of piles supported at bearing bottom layer.

In the traffic-induced vibration problem, the honeycomb WIB measures are investigated as reduction measure. From the analyzed cases, the horizontal response reduction due to horizontal loadings starts at the foundation and extends to the neighborhood, giving almost an effective response reduction above the honeycomb WIB. The honeycomb WIB horizontal length should be sufficient to prevent the possible amplifications at large distances from loading sources. The honeycomb WIB is proved a very promising anti-vibration measure when it is designed properly for the targeted wavelength to be determined from the traffic vibration frequency, structure fundamental vibration mode and the soil condition.

References

1) Kouno, M., Suzuki No, Wada N. and Sakate M., A composite pile foundation with improved soil and its loading test, *Bridge and Foundation Engineering*, Vol. 34, No. 1, pp.21-27, 2000 (in Japanese).
2) Takemiya, H. and Fujiwara, A., Wave propagation/ impediment in a stratum and wave impeding block(WIB) measured for SSI response reduction, *Soil Dynamics and Earthquake Engineering*, Vol. 14, No. 1, pp.49-61, 1994.
3) Takemiya, H., Matsumoto, S., Maekawa, R., Naruse, T., Hosotani, K., Hashimoto M. and Shiraga A., Vibration reduction effect of positive use a wave impeding barrier (WIB), *Proccedings of 34th Japanese Geotechnical Engineering Society Symposium*, Vol. 1, pp.241-242, 1999 (in Japanese).
4) Takemiya, H. and Adam, M., 2D nonlinear seismic ground analysis by FEM-BEM: The case of Kobe in Hyogo-ken Nanbu earthquake, *Proceedings of the JSCE*, No.584/I-42, pp. 19-27, 1998.
5) Giberson, M.F., Two nonlinear beams with definitions of ductility, *Journal of the Structural Division, Proceedings of the American Society of Civil Engineers*, Vol. 95, ST2, pp. 137-157, 1969.
6) Takemiya, H. and Shimabuku, J., Nonlinear seismic damage analysis of bridge pier supported by piles, *The 10th Earthquake Engineering Symposium Proceedings*, Vol. 2, Yokohama, Japan, pp. 1687-1692, 1998.
7) Saidi, M. and Sozen, M. A., Simple and complex models for nonlinear seismic response of reinforced concrete structures, *Structural Research Series No. 465*, Civil Engineering Studies, University of Illinois, Urbana, 1979
8) Shimabuku, J. and Takemiya, H., Nonlinear soil-pile foundation interaction analysis based on FEM-BEM hybrid technique, *Proceedings of the 25th JSCE Earthquake Engineering Symposium*, Tokyo, Japan, pp. 461-464, 1999.
9) Hardin, B.O. and Drnevich, V.P., Shear modulus and damping in soils: design equations and curves, *Journal of the Soil Mechanics and Foundations Division*, ASCE, Vol. 98, SM7, pp. 667-692, 1972.
10) Takemiya, H., Maotian, L. and Gao, L., 2-D nonlinear seismic response of soil structures with emphasis on local topography, *Report submitted to Monbusho International Scientific Research Program*, Grant No. 0104409, 1991.
11) Japan Road Association, *Design Specifications of Highway Bridges, Part IV. Substructure Design*, Maruzen Co., Tokyo, 1996 (in Japanese).
12) Japan Road Association, *Design Specifications of Highway Bridges, Part V. Seismic Design*, Maruzen Co., Tokyo, 1996 (in Japanese).
13) Railway Technical Research Institute, *Seismic Design Code for Railway Structures*, Maruzen Co., Tokyo, 1999 (in Japanese).
14) Shimabuku, J. and Takemiya, H., Inelastic seismic response of bridge piles: effects of superstructure properties and soil layering, *Journal of Structural Mechanics and Earthquake Engineering*, Paper No. 1-221, revised edition submitted in September, 2001.
15) Japan Highway Technical Center, *Structure-Foundation Technical Report of Tokyo Peripheral Motorway*, Tokyo, 2000 (in Japanese).
16) Takemiya, H., Vibration measurement at Shuho Bridge on Route 2 (Okayama Bypass), *Internal Report*, Okayama University, 2000 (in Japanese).

(Received September 14,2001)